

## Chapter 3

# Excited States Calculations for Protonated PAHs

### 3.1 Introduction

Protonated PAHs are closed shell ions. Their electronic structure should therefore be similar to that of neutral PAHs, but as is shown in this chapter, the electronic transitions of protonated PAHs are shifted to the red. The red shift occurs because the HOMO – LUMO gap is reduced due to rehybridization of the protonated carbon atom. Thus, one may expect that even small protonated PAHs would absorb in the visible wavelength range, that is, where the diffuse interstellar bands are located. Based on the assumption that protonated PAHs may be a class of DIB carriers, the experimental measurement of their electronic spectra is an important goal. Before undertaking such experiments, a survey of the expected protonated PAHs excited states could be used to guide the choice of molecules for study, based on the predicted proximity to observed DIBs. *Ab initio* calculations may be very helpful in making such predictions, as well as providing better knowledge of the electronic structure of protonated PAHs. However, it must be realized that such calculations are far from being precise and are best viewed as a guide for further research. Here, the  $S_1$  states are the objects of interest as they participate in the longest wavelength absorption

from the ground electronic state.

## 3.2 Methodology

To calculate the energies of the excited states for neutral and protonated PAHs, the same hardware and software (GAUSSIAN 98, Revision A.9 [98]) were used as in the ground state calculations (Chapter 2). All excited state calculations were performed on geometries that were first optimized at the B3LYP 6-311++G\*\* level.

### 3.2.1 Theory Level and Basis Set

A number of methods have been used to calculate excited states of neutral PAHs and their cations [122–127]. The methods for calculating excited states are not as precise as for the ground state, indeed, they are currently an active area of research. Some are rather complicated and require a careful choice of the orbitals to be considered. The goal of the calculations carried out here is not to predict the positions of each excited state precisely, but rather to estimate where they are located. In addition, information about the *relative* energetics of the same state but in different isomers of protonated PAHs would be very useful as a guide to experiments.

The Configuration Interaction – Singles (CIS) method [122] was used here to perform calculations. This is the least precise excited state method, since it is an analog for the ground state Hartree-Fock method, but it does not require a prior knowledge about the electronic structure of the molecule and is reasonably stable for most molecules. Since protonated PAHs are closed shell species, the CIS method may be applied to them as well.

The choice of calculation parameters was based on the benzene calculation discussed in exercise 9.4 of [128]. The full call for the excited states calculation was:

```
# rCIS=(Direct,Singlets,NStates=12)/6-311++G(2d,2p) Density=Current
IOp(9/40=2) Pop=Full
```

The 6-311++G(2d,2p) basis set was chosen based on the convergence analysis described in 3.2.2. Only singlet states were considered (*Singlets* keyword) as relevant to one-photon electronic absorption spectroscopy. The first twelve singlet excited states were calculated (*NStates=12*). Such a large number was not required, but used to avoid missing any degenerate or forbidden transitions. *Density=Current* was used for better estimates of the oscillator strengths for each transition. *Pop=Full* ensured that all orbitals were considered in the orbital population analysis, and *IOp(9/40=2)* specified which wavefunction coefficients were to be included in the output. The *Direct* keyword was used to avoid problems with disk space for larger molecules.

### 3.2.2 Convergence Tests

The accuracy of the excited states calculation depends on the basis set and the geometry optimization. To investigate the effect of both factors on the first singlet excited state, a number of tests were performed on neutral and protonated naphthalene. A summary of the results is presented in Table 3.1. A general trend is the increase in the wavelength with the increase in the CIS basis set. However, even with the biggest basis set used, the photon energy was overestimated because the experimental value for neutral naphthalene is known to be at a much longer wavelength (312 nm).

For the geometry optimization, tests were carried out with and without diffuse functions, but the difference was found to be negligible (0.06%). The effect of the basis set on CIS energies is seen to be more noticeable. In particular, the addition of both polarized (d,p) and diffuse (+) functions in the basis set improves the performance. The calculated wavelengths

Table 3.1: Convergence dependence on the basis set for the  $S_1 \leftarrow S_0$  transition wavelength (nm) calculations in neutral and protonated naphthalene.

CIS basis set	B3LYP 6-311G(d,p) geom		B3LYP 6-311++G(d,p) geom		
	$C_{10}H_8$	$2-C_{10}H_9^+$	$C_{10}H_8$	$1-C_{10}H_9^+$	$2-C_{10}H_9^+$
3-21G	225.75	329.02			
4-31G	227.82	331.00	228.07	287.02	331.20
6-31G	229.37	332.66	229.62	288.29	332.87
6-31G(d,p)			236.21	294.69	338.55
6-31+G(d,p)			242.13	297.68	341.35
6-31++G(d,p)			242.14	297.80	341.64
6-311G	231.94	334.60	232.20	290.15	334.81
6-311G(d)	239.94	341.31			
6-311G(d,p)	240.24	341.04	240.50	297.08	341.25
6-311+G(d)			243.56	298.48	342.96
6-311+G(d,p)	243.71	342.54	243.97	298.79	342.76
6-311++G(d,p)	243.72	342.66	243.98	298.84	342.88
6-311++G(2d,2p)			245.86	300.55	345.45

appear to group together for minor basis set changes and experience a ‘nudge’ towards smaller energies upon more significant changes. The basis set changes explored were 4-31G  $\rightarrow$  6-31G, 6-31G  $\rightarrow$  6-311G, the addition of polarized functions [105] (either d or d,p), a change in the level of polarized functions (from d,p to 2d,2p), and the addition of at least one diffuse function [106]. With each change, the calculated values move toward the experimental values. From these tests, the 6-31+G(d) basis set appears to be the minimum required for CIS calculations on neutral and protonated PAHs. Here, the 6-311++G(2d,2p) was selected for excited states calculations. This basis set is relatively large, but at the same time, CIS calculations are still significantly faster than geometry optimizations. Typically, 4 hours were needed to calculate the singlet energies and about another 20 hours to perform the population analysis on the P4-2.7 system.

### 3.2.3 Scaling Factors

Clearly, the CIS calculations tend to overestimate the excited states energies. The easiest way to compensate for this in a homologous suite of compounds is an empirical approach, that is, scaling the calculated results to better match experimental values. Fortunately, the gas phase  $S_1 \leftarrow S_0$  transition wavelengths have been measured for many small neutral aromatics (benzene [129], naphthalene [70], anthracene [69], phenanthrene [130,131], pyrene [131,132]). The ratios of the calculated and experimental values are presented in Table 3.2. They lie mainly in the range  $0.77 \pm 0.01$  for all molecules considered, except anthracene (0.846). Based on this result, the scaling factor for protonated PAHs should be somewhere in the 0.75 – 0.85 range. Here, the scaling factors obtained from the respective neutral molecule calculations are used.

Table 3.2: Scaling factors for the  $S_1 \leftarrow S_0$  transitions in neutral aromatic hydrocarbons.

Molecule	$S_1 \leftarrow S_0$ wavelength (nm)		Scaling factor
	Calculated	Experimental	
Benzene (C <sub>6</sub> H <sub>6</sub> )	206.22	262.56	0.78542
Naphthalene (C <sub>10</sub> H <sub>8</sub> )	243.98	312.30	0.78123
Anthracene (C <sub>14</sub> H <sub>10</sub> )	305.39	361.17	0.84556
Phenanthrene (C <sub>14</sub> H <sub>10</sub> )	258.26	340.99	0.75738
Pyrene (C <sub>16</sub> H <sub>10</sub> )	282.19	367.43	0.76801

The validity of scaling down the calculated values may be questioned, especially whether the factor for the neutral molecule can be applied to its protonated versions. To date, experimental data are available only for protonated benzene [89,90]. Calculated but scaled wavelengths for the C<sub>6</sub>H<sub>7</sub><sup>+</sup>  $S_1 \leftarrow S_0$  transition (349.77 nm in Table 3.3) is slightly red-shifter from the experimentally measured band maximum at  $\sim 335$  nm. The scaled predicted and experimental values also turn out to be very close for isomer 1 of protonated anthracene, and somewhat red-shifted for isomer 2 (Chapter 6).

### 3.3 Valence Molecular Orbitals

In neutral aromatic molecules, the transitions from the ground to the first few excited electronic states are  $\pi - \pi^*$  transitions. The electronic structure of protonated PAHs should therefore not differ drastically from neutral PAHs. In particular, their  $S_1 \leftarrow S_0$  transitions should be  $\pi - \pi^*$  as well. To illustrate the changes in the molecular  $\pi$  orbitals upon protonation, the benzene molecule is first considered as an example system.

#### 3.3.1 Protonated Benzene

The benzene molecule is one of the most popular benchmark systems in chemistry. Its molecular orbital system is well-studied and is described in nearly every general chemistry textbook. The molecular  $\pi$  orbitals of neutral benzene based on Hückel theory are shown in Figure 3.1. These are the *NaturalOrbitals* from an energy calculation (HF STO-3G) on previously optimized geometries (B3LYP 6-311++G\*\*) and visualized in Chem3D [133].

Upon protonation, the hybridization of one of the carbon atoms changes from  $sp^2$  to  $sp^3$  (Figure 3.2). As a result, its  $p_z$  orbital is not a part of the aromatic system and the ring is no longer aromatic. The  $p_z$  orbitals of the other five carbon atoms remain unchanged and still form a conjugated system, as can best be seen in the  $2b_2$  orbital that is lying just below the HOMO.

Because of this reduction in symmetry, the orbitals of protonated benzene are no longer degenerate. Two out of the six benzene orbitals (one  $e_{1g}$  and one  $e_{2u}$ ) do not overlap with the protonation site, and therefore have the same appearance in protonated benzene (two  $a_2$  orbitals), with energies that are barely perturbed by protonation. The other four orbitals, however, are altered substantially by the protonation process and become a hybrid of carbon  $p_z$  orbitals and hydrogen  $s$  orbitals (four  $b_2$  orbitals), since the C-H bonds at

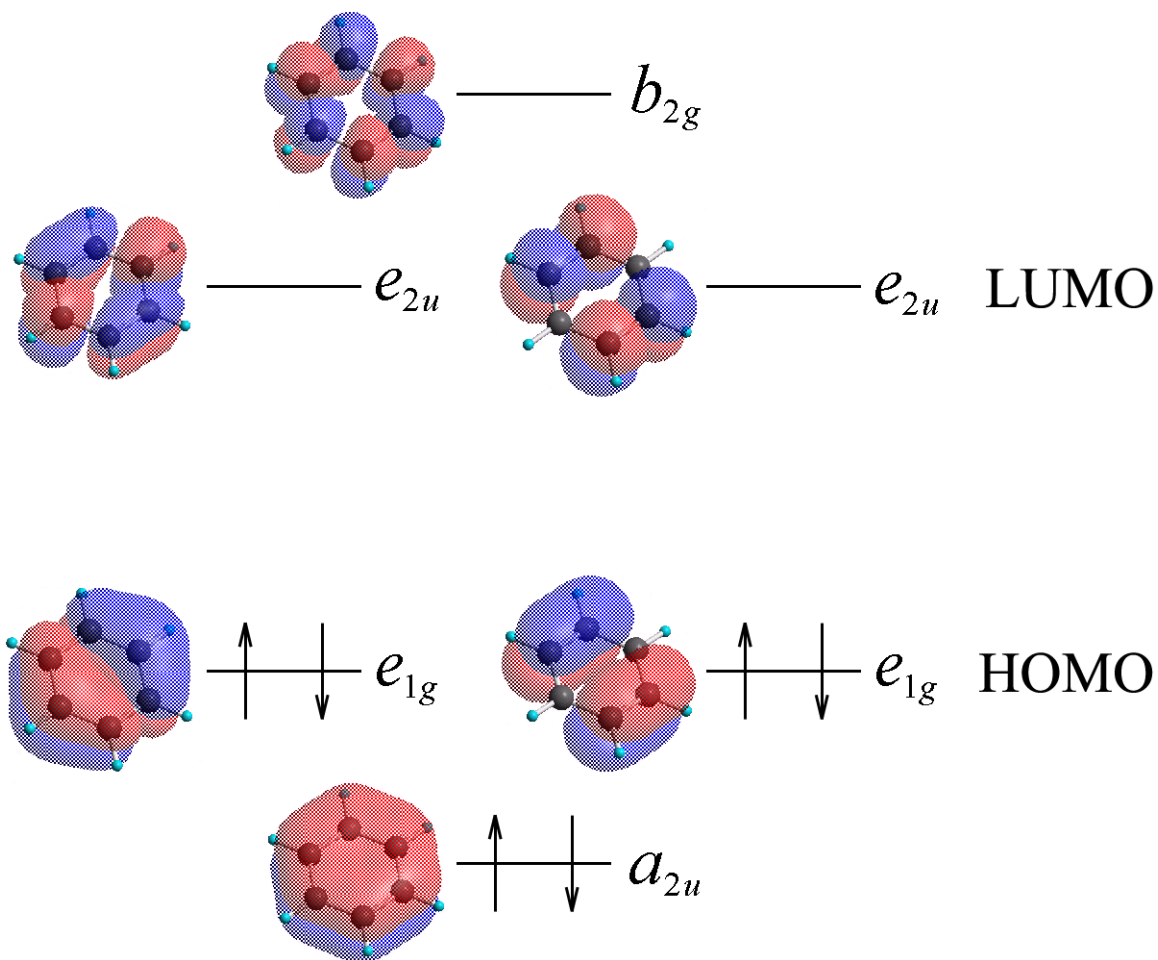


Figure 3.1: The  $\pi$  molecular orbitals of benzene.

the  $\text{CH}_2$  site are  $\sigma$  bonds. As a result, their energies are lowered with respect to neutral benzene orbitals (solid *vs.* dashed lines in Figure 3.2). Since the HOMO is unaffected, this reduces the HOMO – LUMO gap, which leads to a red shift in the absorption spectrum.

### 3.3.2 Other Protonated Aromatics

When a molecule with more than one ring is protonated, the changes in orbitals are similar to benzene, that is, the aromaticity is lost only in the ring with the protonation site while other rings remain aromatic. Unlike the benzene molecule, the HOMOs and

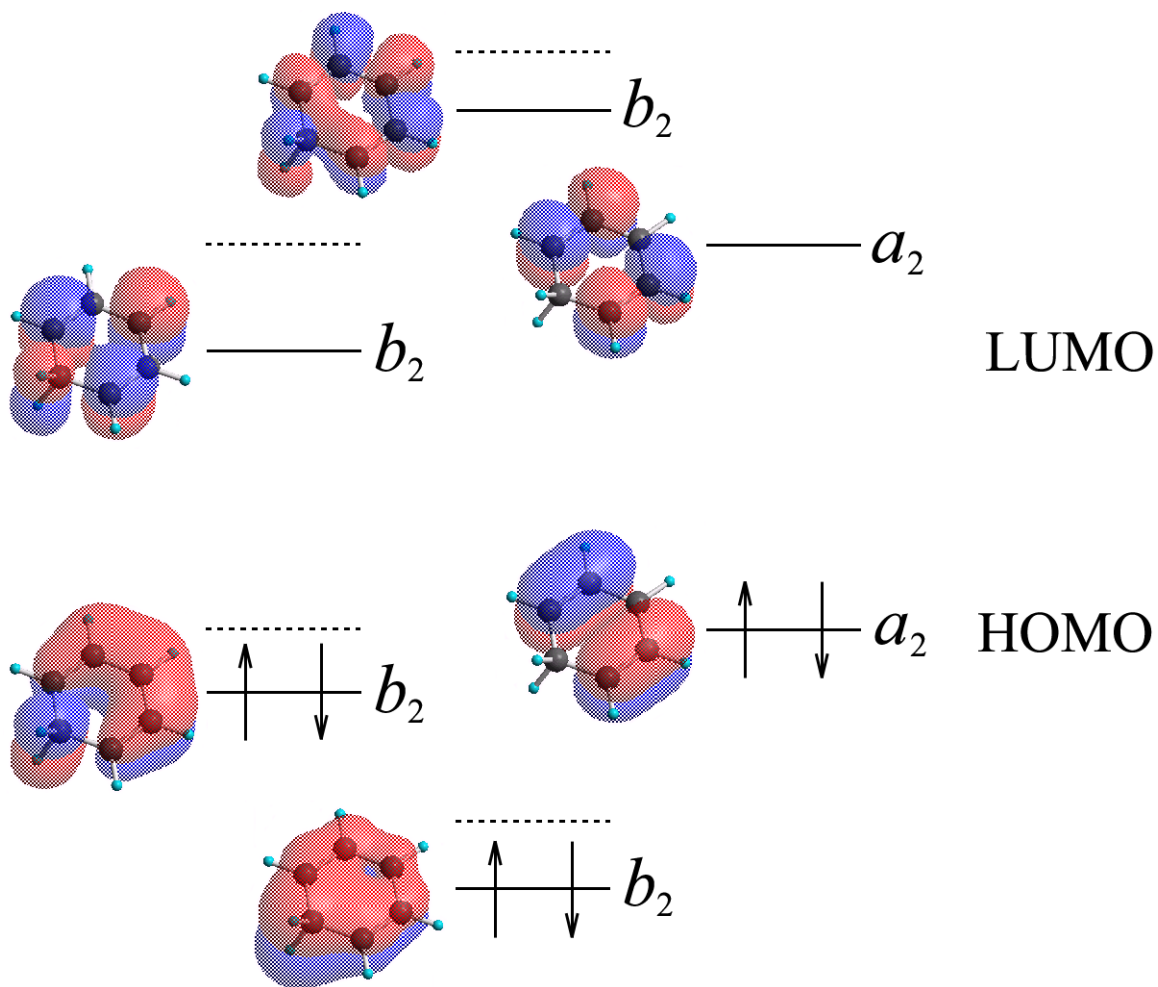


Figure 3.2: The  $\pi$  molecular orbitals of protonated benzene.

LUMOs of neutral polycyclic aromatic molecules are non-degenerate and remain that way after protonation. Orbital images of the HOMOs and LUMOs of neutral and protonated PAHs are shown in Appendix A, Table A.39.

### 3.3.3 Electronic States Assignment

The assignment of electronic states is based on the molecular orbital symmetry [134]. Among neutral PAHs, benzene belongs to the  $D_{6h}$  symmetry group, naphthalene, anthracene and pyrene to the  $D_{2h}$  group, and phenanthrene to the  $C_{2v}$  group. The symmetry



is reduced in protonated PAHs. Protonated benzene, isomer 9 of protonated anthracene and isomer 2 of protonated pyrene are members of the  $C_{2v}$  symmetry group, while the rest have  $C_s$  symmetry.

The exact assignment of the orbital symmetry depends on the choice of the orthogonal coordinate system. Here, for all non- $C_{2v}$  symmetric molecules, the Z axis is set to be normal to the molecular plane by analogy with neutral benzene (Figure 3.3 **1**). In molecules with  $C_{2v}$  symmetry, the Z axis is selected as the rotational  $C_2$  symmetry axis (Figure 3.3 **2**), with the X axis set orthogonal to the Z axis in the molecular plane and in the prolate direction. The Y axis is orthogonal to the X and Z axes. It is therefore in the molecular plane for non- $C_{2v}$  symmetric molecules. This coincides with the coordinate system used in studies of the valence states of polyacenes [127].

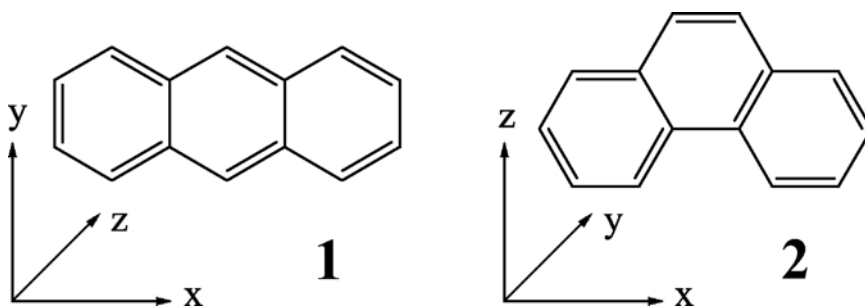


Figure 3.3: Orthogonal axis selection for molecules with different symmetry.

Based on this coordinate system, the ground and the first singlet electronic states, as well as electronic configurations, were assigned (Appendix A, Table A.38). The total number of  $\pi$  orbitals was the same as the number of carbon atoms. The symmetries of orbitals were determined by visual inspection. The electronic states were then labeled using the symmetry of HOMO and LUMO orbitals (the ones that have  $x$  and  $y$  electrons in Table A.38).

$C_s$ -symmetric molecules (the majority of protonated PAHs) present the simplest case. For them, all orbitals have  $a''$  symmetry. Thus, the ground state ( $S_0$ ) is  $\tilde{X}^1A'$  and the first singlet excited state ( $S_1$ ) is  $\tilde{A}^1A'$ . For  $C_{2v}$ -symmetric molecules, the HOMOs and LUMOs have  $a_2$  and  $b_2$  symmetry, leading to  $\tilde{X}^1A_1$  ground states and to  $\tilde{A}^1B_1$  for  $S_1$  states. The orbital symmetries become more diverse for  $D_{xh}$ -symmetric molecules. Molecules with  $D_{2h}$  symmetry have  $\tilde{X}^1A_g$   $S_0$  states and  $\tilde{A}^1B_{xu}$  ( $x = 1, 2$  or  $3$ )  $S_1$  states. For the benzene molecule ( $D_{6h}$ ), it is well known that the  $S_0$  state is  $\tilde{X}^1A_{1g}$  and the  $S_1$  state is  $\tilde{A}^1E_{1u}$ .

### 3.4 Excited States Energies

The first singlet excited state energies and  $S_1 \leftarrow S_0$  transition wavelengths were calculated for the neutral and stable isomers of protonated benzene, naphthalene, anthracene, phenanthrene, and pyrene. A short overview of the results is presented in Table 3.3, and the full version is presented in Appendix A, Table A.37. The wavelengths in both tables are scaled by the neutral PAHs experimental values. The scaling in Table A.37 ranges for 0.75 – 0.85.

As one would expect, the  $S_1 \leftarrow S_0$  wavelengths for protonated PAHs are shifted to the red, as compared to their neutral PAH precursors. There is a wide range of red shifts, from 15 nm for isomer 9 of protonated anthracene to just over 200 nm for isomer 2 of protonated pyrene. The majority are significant, on the order of 100 nm (Appendix A, Table A.37).

The  $S_1 \leftarrow S_0$  transitions for small neutral PAHs lie at UV wavelengths range, and so are not important to the DIBs. With the exception of protonated benzene, however, all of the protonated versions of small PAHs have isomers that should absorb visible wavelength photons. In fact, all isomers of protonated phenanthrene and pyrene absorb in the visible. Roughly, it appears that the closer the protonation site is to the center-of-mass of the

Table 3.3: Scaled calculated  $S_1 \leftarrow S_0$  wavelengths for neutral and protonated PAHs.

Molecule	$S_1 \leftarrow S_0$ Wavelength (nm)
<b>Benzene</b>	
$C_6H_6$	262.56
$C_6H_7^+$	349.77
<b>Naphthalene</b>	
$C_{10}H_8$	312.30
1- $C_{10}H_9^+$	382.53
2- $C_{10}H_9^+$	438.90
<b>Anthracene</b>	
$C_{14}H_{10}$	361.17
1- $C_{14}H_{11}^+$	443.09
2- $C_{14}H_{11}^+$	490.41
9- $C_{14}H_{11}^+$	376.47
<b>Phenanthrene</b>	
$C_{14}H_{10}$	340.99
1- $C_{14}H_{11}^+$	477.20
2- $C_{14}H_{11}^+$	497.78
3- $C_{14}H_{11}^+$	460.81
4- $C_{14}H_{11}^+$	493.13
9- $C_{14}H_{11}^+$	479.36
<b>Pyrene</b>	
$C_{16}H_{10}$	367.43
1- $C_{16}H_{11}^+$	442.82
2- $C_{16}H_{11}^+$	569.30
4- $C_{16}H_{11}^+$	499.23

molecule, the shorter the wavelength of the  $S_1 \leftarrow S_0$  transition. For polyacenes (naphthalene, anthracene), this also correlates with isomer ground state stability; more stable isomers absorb at shorter wavelengths.

The photon energies for the  $S_1 \leftarrow S_0$  transitions are close to the ground state dissociation thresholds for protonated PAHs calculated in Chapter 2 (Table 3.4). After absorbing a UV/visible photon, the protonated PAH ion ends up in an electronically excited state that may undergo an internal conversion to the ground electronic state. The photon energy in this case would be converted into vibrations via intramolecular vibrational energy redistribution (IVR). This means that protonated benzene, naphthalene and anthracene would, in

principle, have enough energy to dissociate even when excited to the  $S_1$  electronic state. Larger protonated PAHs would have enough energy to dissociate when excited to higher electronic states. Thus, it may be possible to record absorption spectra of protonated PAHs by resonance-enhanced dissociation method. Such an attempt is made in Chapter 5. At the same time, this casts a shadow on the prospective of protonated PAHs survival in the interstellar medium.

Protonated PAHs are expected to be strong absorbers, since the calculated oscillator strengths for the  $S_1 \leftarrow S_0$  transitions are in the 0.14 – 0.7 range (Appendix A, Table A.37). Depending on the isomer, some of them may absorb better than their neutral cousins.

Table 3.4: Comparison of the calculated  $S_1 \leftarrow S_0$  wavelengths and ground state dissociation energies for protonated PAHs, in kcal/mol.

Molecule	$S_1 \leftarrow S_0$ Wavelength	Dissociation Energy
<b>Benzene</b>		
$C_6H_7^+$	81.74	63.22
<b>Naphthalene</b>		
1- $C_{10}H_9^+$	74.32	62.41
2- $C_{10}H_9^+$	64.66	59.51
<b>Anthracene</b>		
1- $C_{14}H_{11}^+$	64.53	52.41
2- $C_{14}H_{11}^+$	58.30	49.36
9- $C_{14}H_{11}^+$	75.95	61.06
<b>Phenanthrene</b>		
1- $C_{14}H_{11}^+$	59.92	59.53
2- $C_{14}H_{11}^+$	57.44	57.53
3- $C_{14}H_{11}^+$	62.05	58.98
4- $C_{14}H_{11}^+$	57.98	58.46
9- $C_{14}H_{11}^+$	59.64	59.33
<b>Pyrene</b>		
1- $C_{16}H_{11}^+$	64.57	60.78
2- $C_{16}H_{11}^+$	50.22	46.57
4- $C_{16}H_{11}^+$	57.27	50.52

### 3.4.1 Comparison with DIB spectrum

Since protonated PAHs are predicted to be strong absorbers of visible wavelength photons, it is interesting to compare calculated  $S_1 \leftarrow S_0$  transition wavelengths with the spectrum of the diffuse interstellar bands. The DIB synthetic absorption spectrum is calculated based on extensive DIB surveys [31–33] that were compiled from many different astronomical sources [1]. In Figure 3.4, the black solid line is the synthetic DIB spectrum; vertical colored dashed lines are the scaled  $S_1 \leftarrow S_0$  wavelengths; and the horizontal colored solid lines are the scaled wavelengths ranges for each transition.

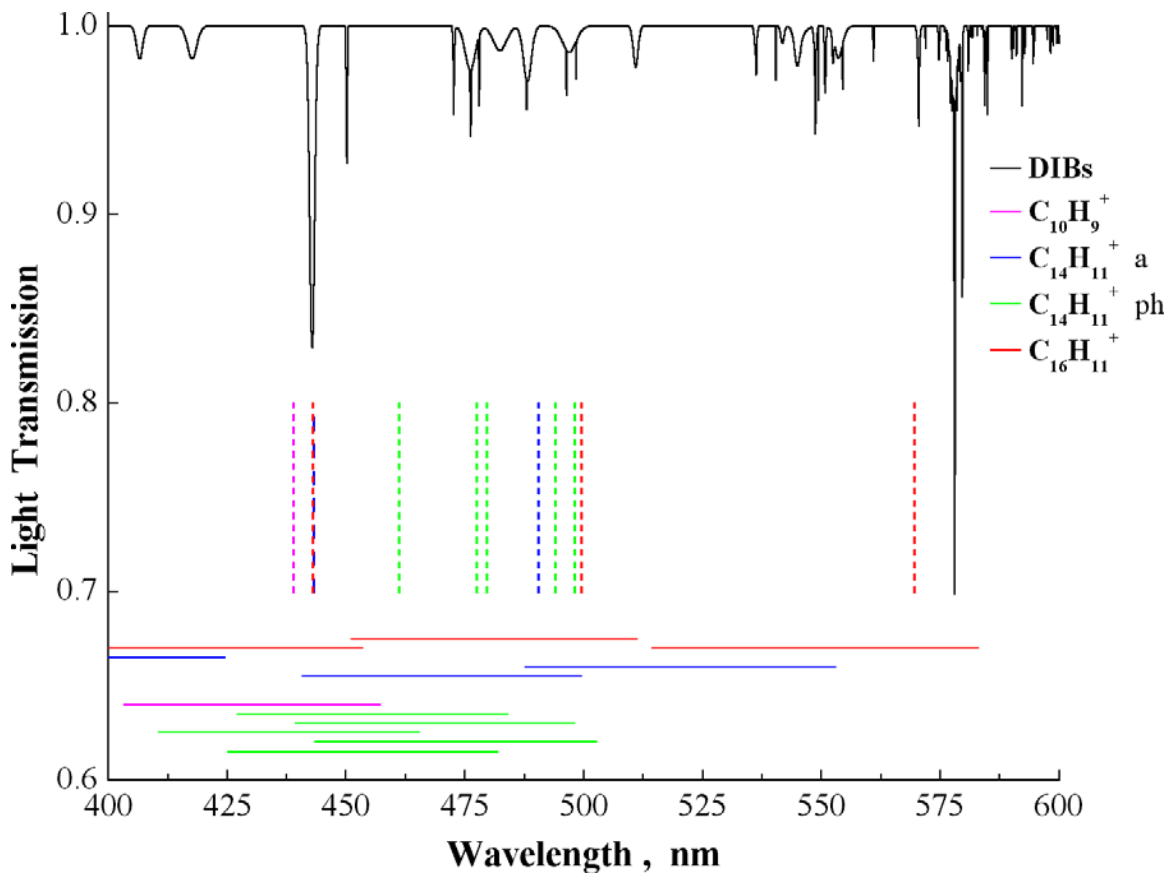


Figure 3.4: Diffuse interstellar bands and calculated  $S_1 \leftarrow S_0$  wavelengths for protonated PAHs.

Since protonated PAHs are relatively large molecular ions, their absorption bands should be broader than for small molecules. Hence, if protonated PAHs are the DIB carriers, they should contribute to broad DIB features (1 – 3 nm wide). There are three different protonated PAH isomers (from naphthalene, anthracene and pyrene) that absorb near the strong 443 nm band. Four isomers of protonated phenanthrene and one from protonated anthracene and pyrene should absorb in 470 – 520 nm range, where five broad bands are located. One isomer of protonated pyrene is in the vicinity of the 578 nm band. The proximity of the calculated transitions to the broad DIBs makes a good argument in favor of protonated PAHs as DIB carriers, however, it should be tested experimentally. The UV/visible absorption spectra of protonated PAHs in the gas phase need to be measured. This issue is addressed in Chapters 5 and 6.

### 3.5 Summary

$S_1 \leftarrow S_0$  transition wavelengths were calculated for neutral and protonated PAHs with CIS method. The symmetries of the ground and the first singlet excited states were assigned together with their electronic configurations. It was determined that most protonated PAHs have  $\tilde{X}^1A'$  ground state and  $\tilde{A}^1A'$  excited  $S_1$  state.

The  $S_1 \leftarrow S_0$  transitions for most protonated PAHs are estimated to be in the visible, where the DIBs are located. They are fairly close to a number of the broad DIB features. This is encouraging news for the theory that protonated PAHs are DIB carriers. For species with a few isomers in the DIB range, the match of a few experimentally measured bands with DIBs would be solid proof for such a theory.

The energy differences between LUMO and HOMO in protonated PAHs are close to their dissociation thresholds. In the absence of IVR, this makes them potentially unstable

in the ISM, but as the size of the molecule gets larger, IVR has a profound effect on the stabilization of PAHs. As was found in Chapter 5, even relatively small protonated PAHs may be photostable in the ISM.